Combined Static-Time-Harmonic Finite Element Method to Simulate Eddy Currents in the Permanent Magnets of a Synchronous Machine

Herbert De Gersem, Kay Hameyer, Thomas Weiland

Abstract— **Eddy current losses in the rare-earth permanent magnets mounted on the rotor of of permanent magnet machine are computed using a hybrid static-time-harmonic, field-circuit coupled finite element method. The air gap field generated by the stator windings is transformed in Fourier components. The synchronously rotating component is forwarded to a static rotor model accounting for the remanent field of the magnets whereas relevant higher harmonic components are propagated towards additional rotor models with equivalent non-magnetized magnet material properties. The time-harmonic rotor models consider the eddy currents in the conductive magnet material induced by a set of higher order harmonic field components at a corresponding slip frequency. Ferromagnetic saturation mutually influences the rotor models and is resolved by a successive approximation scheme. The combined static-time-harmonic finite element approach is applied to a permanent magnet synchronous machine.**

Index terms—**finite element methods, eddy currents, moving bodies, permanent magnet synchronous machines**

I. INTRODUCTION

TO design permanent magnet (PM) synchronous machines (SMs) one relies upon stationary characteristics such as the dependence of the electromotive force, the mechanic force and the stator winding inductances on the load angle [1]. Accurate data can be provided by static finite element (FE) simulation accounting for the magnetisation of the magnets and the ferromagnetic saturation of the iron parts [2], [3]. This approach, however, neglects important secondary effects such as eddy current losses in the PMs and rotor core (if the rotor is not laminated), which are responsible for saturation effects and heating. Especially NdFeB and SmCo PMs suffer from significant eddy current losses and are particularly sensible for temperature degradation. To deal with these effects, commonly, the static FE method is replaced by transient simulation [4], [5]. A transient analysis is, however, considerably more expensive and therefore not recommended within design procedures. Another possibility consists of computing secondary effects by post-processing a previously obtained static FE solution [6]. This approach does not account for coupled effects, such as e.g. the influence of additional ferromagnetic saturation due to eddy currents in the PMs on the global flux linkage between stator and rotor.

In this paper, eddy currents are considered by a static-time-harmonic coupled model simulating the stationary behaviour without time stepping. The stationary behaviour is preserved in the formulation and is exploited in the FE model. The approach offers more favourable simulation times when compared to transient FE analysis. Coupled effects such as ferromagnetic saturation and external circuit connections are adequately resolved by the FE model.

H. De Gersem and T. Weiland are with the Technische Universität Darmstadt, Computational Electromagnetics Laboratory, Schloßgartenstraße 8, D-64289 Darmstadt, Germany (e-mail: degersem/weiland@temf.tu-darmstadt.de).

K. Hameyer is with the Katholieke Universiteit Leuven, Dep. ESAT, Div. ELECTA, Kasteelpark Arenberg 10, B-3001 Leuven-Heverlee, Belgium (e-mail: kay.hameyer@esat.kuleuven.ac.be).

H. De Gersem is working in the cooperation project "DA-WE1 (TEMF/GSI)" with the "Gesellschaft für Schwerionenforschung (GSI)" Darmstadt.

II. AIR-GAP FIELD COMPONENTS

The three-phase winding of the SM stator is excited by a sinusoidal three-phase voltage source at frequency f. Due to the distributed stator winding and due to the slotting of stator and rotor, the magnetic field in the air gap contains, besides the fundamental rotating field at sychronous speed, higher harmonic fields. The synchronously rotating magnetic flux density in the air gap is

$$B_{\mathrm{st},1}(\theta,t) = \mathrm{Re}\left\{\underline{b}_1 e^{\jmath(\omega t - p\theta)}\right\} \tag{1}$$

with $\omega = 2\pi f$ the electrical pulsation, p the pole pair number of the SM and θ the angular coordinate in the air gap. Higher spatial harmonic components are written by

$$B_{\mathrm{st},\lambda}(\theta,t) = \mathrm{Re}\left\{\underline{b}_\lambda e^{\jmath(\omega t - p\lambda\theta)}\right\} \tag{2}$$

with λ the harmonic order. If the SM rotates at the synchronous speed $\omega_m = \omega/p$, an observer attached to the moving rotor experiences the air gap field (1) as a static field:

$$B_{\mathrm{rt},1}(\theta') = \mathrm{Re}\left\{\underline{b}_1 e^{-\jmath p\theta'}\right\} . \tag{3}$$

with θ' the angular coordinate with respect to the rotor observer. This fact motivates the use of static FE models to simulate SMs operating at steady state. Static FE models allow to determine basic lumped parameters such as direct and quadrature axis inductances, leakage inductances, electromotive forces and torques and their dependence on the load angle [7], [8]. In such static FE models, higher harmonic air-gap field components are treated as static components as well. In reality, however, these components are time-varying fields, also when observed from the rotor:

$$B_{\mathrm{rt},\lambda}(\theta',t) = \mathrm{Re}\left\{\underline{b}_\lambda e^{\jmath\left(\omega_\lambda t - p\lambda\theta'\right)}\right\} . \tag{4}$$

Here, $\omega_\lambda = \omega - p\lambda\omega_m$ are called the *slip pulsation* with respect to the harmonic component of order λ. These time-varying higher harmonic air-gap fields induce eddy currents in the conductive PM material. The FE model developed here, incorporates a spectral decomposition of the air-gap flux, separating the higher-harmonic components from the synchronous component such that eddy current effects can be taken into account.

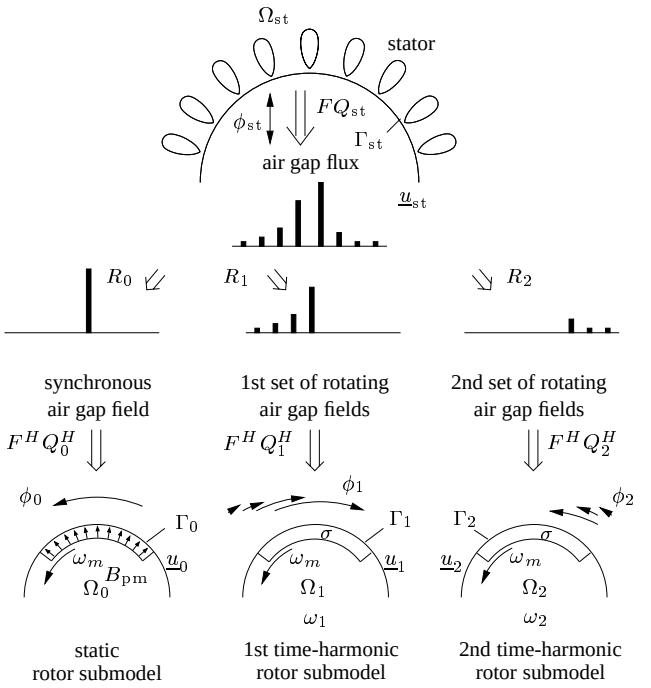

Fig. 1. Combined static-time-harmonic finite element method illustrated for a 2-pole PMSM with $\phi_{\rm st}$ the global air-gap flux, ϕ_0 the synchronously rotating air-gap flux and ϕ_1 and ϕ_2 two sets of higher harmonic air-gap field components.

III. FINITE ELEMENT FORMULATION

The concept of the combined static-time-harmonic method is illustrated by Fig. 1. The global geometry is split up in a stator and rotor part sharing a common arc or circle Γ in the middle of the air gap. A single stator model part $\Omega_{\rm st}$ and $n_{\rm rt}+1$ independent rotor model parts Ω_s ($s=0,\dots n_{\rm rt}$) are considered. In this section, the FE formulations for the individual model parts are described. The next section is devoted to the coupling of the formulations at the interface Γ.

A formulation in terms of the magnetic vector potential $\mathbf{A}$ is applied. Thanks to the symmetry of the geometry, the excitation and the motion of the model, cartesian 2D models in term of the z-component A_z of $\mathbf{A}$ yield a sufficient accuracy. Only steady-state operating conditions are simulated. This allows to confine the formulation to static and time-harmonic partial differential equations (PDEs). In the stator model $\Omega_{\rm st}$, the PDE is

$$-\frac{\partial}{\partial x}\left(\nu\frac{\partial \underline{A}_{\rm st}}{\partial x}\right)-\frac{\partial}{\partial y}\left(\nu\frac{\partial \underline{A}_{\rm st}}{\partial y}\right)-\sum_{k=1}^{3} g_k(x,y)\underline{I}_k=0 \quad (5)$$

with ν the reluctivity, $\underline{A}_{\rm st}$ the phasor of A_z with respect to the pulsation ω, $\underline{I}_k$ the current in stator winding k and $g_k(x,y)$ a function representing the current density distribution in $\Omega_{\rm st}$ due to a unit current in stator winding k. The static rotor model is denoted by Ω_0 and obeys the PDE

$$-\frac{\partial}{\partial x}\left(\nu\frac{\partial A_0}{\partial x}\right)-\frac{\partial}{\partial y}\left(\nu\frac{\partial A_0}{\partial y}\right)=\frac{\partial\left(\nu B_{{\rm pm},y}\right)}{\partial x}-\frac{\partial\left(\nu B_{{\rm pm},x}\right)}{\partial y} \quad (6)$$

with A_0 representing A_z in the static rotor model and $(B_{pm,x}, B_{pm,y})$ the remanent magnetic flux density of the PMs.

The PDEs in the other rotor models Ω_s ($s=1,\dots,n_{\rm rt}$) are

$$-\frac{\partial}{\partial x}\left(\nu\frac{\partial \underline{A}_s}{\partial x}\right)-\frac{\partial}{\partial y}\left(\nu\frac{\partial \underline{A}_s}{\partial y}\right)+\jmath\omega_s\sigma\underline{A}_s -\sum_{q=1}^{n_{\rm pm}}\frac{\sigma}{\ell_z}\Delta\underline{V}_{s,q}=0 \quad (s=1,\dots,n_{\rm rt}) \quad (7)$$

with $\underline{A}_s$ the phasor of A_z with respect to the slip pulsation ω_s in Ω_s, ℓ_z the length of the 2D model, $n_{\rm pm}$ the number of PMs and $\Delta\underline{V}_{s,q}$ the voltage drop in the z-direction along the PM q in rotor model Ω_s.

The PDEs (5), (6) and (7) are discretised by linear, triangular FEs $N_i(x,y)$ yielding $n_{\rm rt}+2$ independent systems of equations

$$K_{\Omega_{\rm st}}\underline{a}_{\rm st}-P\underline{I} = 0\,; \quad (8)$$

$$K_{\Omega_0}a_0 = f_{\Omega_0}\,; \quad (9)$$

$$\left(K_{\Omega_s}+L_{\Omega_s}\right)\underline{a}_s+Q_s\Delta\underline{V}_s = 0 \quad (10)$$

with matrix entities

$$K_{\Omega,i,j} = \int_\Omega \nu\left(\frac{\partial N_i}{\partial x}\frac{\partial N_j}{\partial x}+\frac{\partial N_i}{\partial y}\frac{\partial N_j}{\partial y}\right)\mathrm{d}\Omega\,; \quad (11)$$

$$L_{\Omega_s,i,j} = \int_\Omega \jmath\omega_s\sigma N_iN_j\mathrm{d}\Omega\,; \quad (12)$$

$$P_{i,k} = \int_{\Omega_{\rm st}} g_k(x,y)N_i\mathrm{d}\Omega\,; \quad (13)$$

$$Q_{s,i,q} = \int_{\Omega_{s,{\rm pm},q}}\frac{\sigma}{\ell_z}N_i\mathrm{d}\Omega\,; \quad (14)$$

$$f_{\Omega_0} = \int_{\Omega_0}\left(-\nu B_{{\rm pm},y}\frac{\partial N_i}{\partial x}+\nu B_{{\rm pm},x}\frac{\partial N_i}{\partial y}\right)\mathrm{d}\Omega \quad (15)$$

with $\Omega_{s,{\rm pm},q}$ the cross-section of PM q in Ω_s. The vectors $\underline{a}_{\rm st}$, a_0 and $\underline{a}_s$ contain the degrees of freedom for $\underline{A}_{\rm st}$, A_0 and $\underline{A}_s$. The vectors $\underline{I}$ and $\Delta\underline{V}_s$ contain all $\underline{I}_k$ and $\Delta\underline{V}_{s,q}$ respectively. The systems of FE equations (8) are further concatenated into the block system

$$K\underline{a}+Q\Delta\underline{V}-P\underline{I}=\underline{f}\,. \quad (16)$$

IV. DECOMPOSITION OF THE AIR-GAP FLUX

The boundary Γ is shared by all submodels. In the following, Γ will be denoted more specifically by $\Gamma_{\rm st}$ and Γ_s to distinguish between the sides belonging to the stator submodel $\Omega_{\rm st}$ and the different rotor submodels Ω_s. In the FE formulation developed above, homogeneous Neumann boundary conditions are assumed at $\Gamma_{\rm st}$ and Γ_s. As a consequence, each model part features a set of degrees of freedom at Γ_s. This redundancy has to be elimated by an appropriate set of interface conditions between $\Gamma_{\rm st}$ and Γ_s ($s=0,\dots,n_{\rm rt}$). For convenience and computational efficiency, it is supposed that the grids at $\Gamma_{\rm st}$ and Γ_s are matching and equidistant. The operators $Q_{\rm st}$, Q_0 and Q_s restrict $\underline{a}_{\rm st}$, a_0 and $\underline{a}_s$ to Γ, Γ_0 and Γ_s and, in case of anti-symmetric motor models, complete the restricted sets of degrees of freedom to periodic signals. The resulting vectors represent periodic air-gap fields and are denoted by $\underline{u}_{\rm st}$, u_0 and $\underline{u}_s$:

$$\underline{u}_{\rm st} = Q_{\rm st}\underline{a}_{\rm st}\,; \quad (17)$$

$$u_0 = Q_0a_0\,; \quad (18)$$

$$\underline{u}_s = Q_s\underline{a}_s\,. \quad (19)$$

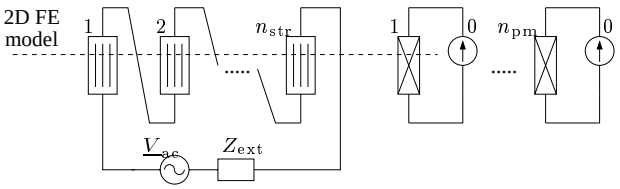

Fig. 2. External electric circuit connection of the PMSM, shown for 1 stator phase and 1 rotor model.

The size of $\underline{u}_{\rm st}$, u_0 and $\underline{u}_s$ is denoted by $n_{\rm fft}$ and determines the size of the Fast Fourier Transform F applied to transform the field distributions along the air gap into spatial harmonic components:

$$\underline{c}_{\rm st} = F\underline{u}_{\rm st}\ ; \tag{20}$$

$$\underline{c}_0 = Fu_0\ ; \tag{21}$$

$$\underline{c}_s = F\underline{u}_s\ . \tag{22}$$

The distribution of particular harmonic components to specific rotor models is represented by a set of restriction operators R_s ($s=0,\ldots,n_{\rm rt}$). Each R_s is a diagonal matrix of size $n_{\rm fft}\times n_{\rm fft}$ selecting a number of harmonics. The sum of all R_s has to be the identity operator in order to preserve the magnetic flux in the air gap. The operator R_0 additionally maps the rotating field represented by the phasor $\underline{c}_0$ upon a static field with the same load angle and thus prevents time-varying flux to enter the static rotor model. The air-gap flux splitting interface conditions read $\underline{c}_s = R_s\underline{c}_{\rm st}$ and are gathered in the constraint equations

$$\underbrace{\begin{bmatrix} R_0FQ_{\rm st} & -FQ_0 & 0 \\ R_sFQ_{\rm st} & 0 & -FQ_s \end{bmatrix}}_{B} \begin{bmatrix} \underline{a}_{\rm st} \\ a_0 \\ \underline{a}_s \end{bmatrix} = \begin{bmatrix} 0 \\ 0 \\ 0 \end{bmatrix}\ . \tag{23}$$

These interface conditions are combined with the FE formulations into the saddle-point problem

$$\begin{bmatrix} K & B^H \\ B & 0 \end{bmatrix} \begin{bmatrix} \underline{a} \\ \underline{\xi} \end{bmatrix} + \begin{bmatrix} Q & -P \\ 0 & 0 \end{bmatrix} \begin{bmatrix} \Delta\underline{V} \\ \underline{I} \end{bmatrix} = \begin{bmatrix} \underline{f} \\ 0 \end{bmatrix} \tag{24}$$

with $\underline{\xi}$ a set of Lagrange multipliers. The term B^H is related to the magnetic field strengths at Γ_s.

The slip pulsation ω_s applied in (7) is chosen to be the slip pulsation associated with the most dominant harmonic component selected by R_s. As a consequence, eddy current effects generated by this component are correctly taken into account whereas eddy currents due to the other components that are selected by R_s are only considered approximately. A conscientious choice of the spectral partitioning and the corresponding slip pulsations, keeps the introduced errors acceptable. If other harmonics turn out to be important as well, an additional rotor model $\Omega_{n_{\rm rt}+1}$ equipped with an appropriate selector $R_{n_{\rm rt}+1}$ and slip pulsation $\omega_{n_{\rm rt}+1}$, can be inserted in the FE model.

V. FIELD-CIRCUIT COUPLING

The fields for the magnetic vector potential are coupled to the stator windings and the PMs by an external electric circuit (Fig. 2). If the stator windings are current driven and the PMs are not conductive, the terms $P\underline{I}$ and $Q\Delta\underline{V}$ are known. Here, however, the stator windings are voltage driven and the voltage drops along the PMs are unknown. A field-circuit coupling scheme is used to add a few circuit equations to the FE system of equations [9].

The voltage drop along stator winding k is equalled to the supply voltage $\underline{V}_{\rm ac}$:

$$R_k\underline{I}_k + \ell_z\int_{\Omega_{\rm st}} g_k(x,y)\jmath\omega\underline{A}_{\rm st}{\rm d}\Omega = \underline{V}_{\rm ac} \tag{25}$$

with R_k the DC resistance of winding k. The last term in (25) represents the induced voltage. The total current in each PM in each of the rotor models is forced to zero:

$$G_{{\rm pm},q}\Delta\underline{V}_{s,{\rm pm},q} - \int_{\Omega_{s,{\rm pm},q}} \jmath\omega_s\sigma\underline{A}_s = 0 \tag{26}$$

with

$$G_{{\rm pm},q} = \frac{\sigma S_{{\rm pm},q}}{\ell_z} \tag{27}$$

the DC conductance and $S_{{\rm pm},q}$ the cross-section of PM q. The coupled system of equations is

$$\begin{bmatrix} K & Q & P & B^H \\ Q^T & \chi_sG & 0 & 0 \\ P^T & 0 & -\chi Z & 0 \\ B & 0 & 0 & 0 \end{bmatrix} \begin{bmatrix} \underline{a} \\ \Delta\underline{V} \\ \underline{I} \\ 0 \end{bmatrix} = \begin{bmatrix} \underline{f} \\ -\chi_s\underline{I} \\ \chi\underline{V} \\ 0 \end{bmatrix} \tag{28}$$

with G and R diagonal matrices containing all $G_{{\rm pm},q}$ and R_k. The diagonal matrices χ_s and χ have entities $1/\jmath\omega_s\ell_z$ and $1/\jmath\omega\ell_z$ respectively. They are inserted to symmetrize the circuit equations according to the FE equations. A more general field-circuit coupling scheme is described in [9] and has been applied to models with air gap flux splitting in [10].

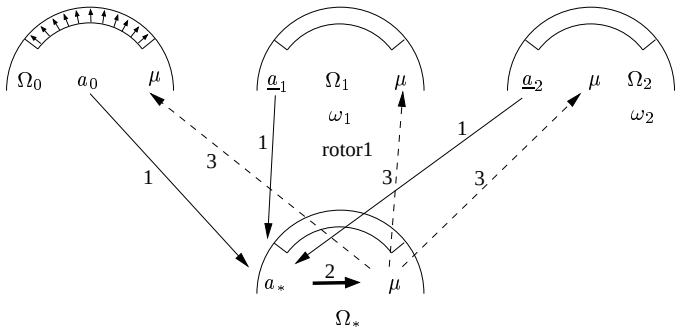

Fig. 3. Successive substitution approach updating the permeabilities of the rotor submodels.

VI. FERROMAGNETIC SATURATION

The static and time-harmonic models are mutually influenced by ferromagnetic saturation. Between two successive linear steps, the true rotor solution $\underline{a}_*$ is reconstructed at an additional rotor submodel by summing all contributions of the rotor models (step 1 in Fig. 3):

$$\underline{a}_* = a_0 + \sum_{s=1}^{n_{\rm rt}} \underline{a}_s\ . \tag{29}$$

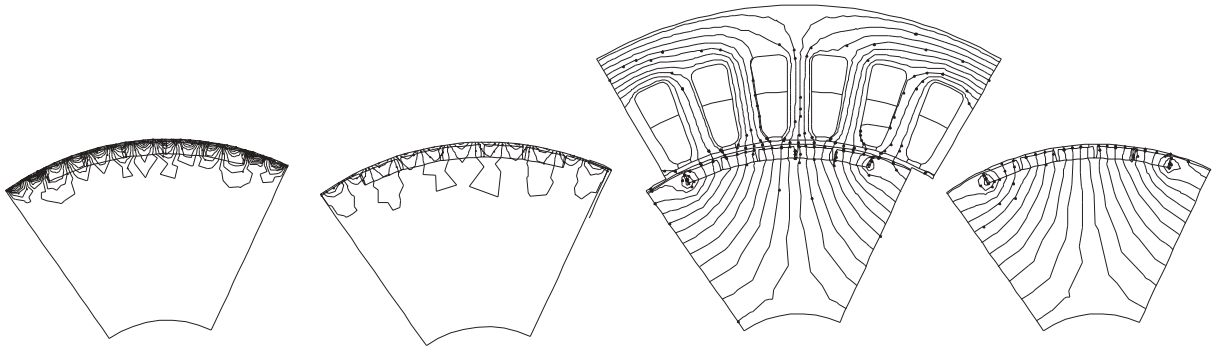

Fig. 4. One pole FE model of a PMSM with (right) a static rotor model, (left) two time-harmonic rotor models and (middle) the true solution in stator and rotor.

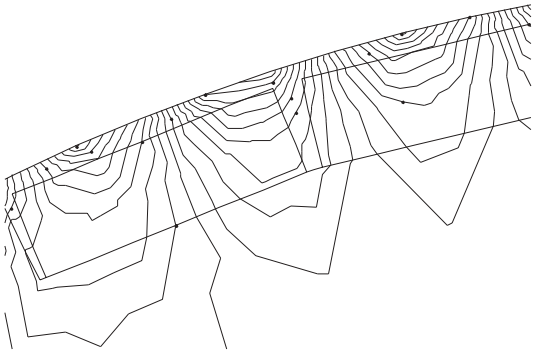

Fig. 5. Detail of the tooth ripple magnetic field in the inset NdFeB magnets of the SM.

The true solution is used to determine a new working point in the non-linear analysis. The value for the permeability in a FE is updated based on the magnitude of the magnetic flux density computed from $\underline{a}_*$ (step 2). This set of permeabilities is applied to all rotor models (step 3). The matrix K in (28) is recalculated and a next successive approximation step is performed.

VII. APPLICATION

The combined static-time-harmonic method is applied to a six-pole 3 kW synchronous machine with NdFeB inset magnets. Only one pole of the motor cross-section is modelled (Fig. 4). At an arc in the middle of the air gap, the air-gap flux is decomposed in harmonic components. The synchronously rotating flux is propagated to the static rotor model (most right in Fig. 4). The most important higher harmonics are those with orders 11th and 13th due to the slotting of the stator. The 11th harmonic component is forwarded to a separate rotor model (second rotor model in Fig. 4). All other harmonics are propagated towards the most left rotor model. The rotor model connected to the stator reflects the true solution which is also used to determine the saturation pattern. The FE model incorporates voltage-driven stator windings fed by a three-phase alternating current source. A detail of the tooth ripple magnetic field is shown in Fig. 5.

VIII. CONCLUSIONS

The spectral decomposition of the air gap field allows to distribute static and time-varying field components to different rotor submodels. A static rotor submodel deals with the remanence of the permanent magnets whereas time-harmonic rotor submodels are applied to compute the currents induced in the conductive magnet material due to higher harmonic air gap fields. Ferromagnetic saturation and field-circuit coupling are considered. The application of the method to a permanent magnet synchronous machine indicates the convenience and efficiency of the method for computing steady-state operating conditions including eddy current effects in permanent magnet material.

REFERENCES

[1] K. Vogt, *Elektrische Maschinen, Berechnung rotierender elektrischer Maschinen*, Verlag Technik Berlin, 2 edition, 1974.

[2] S. Henneberger, U. Pahner, K. Hameyer, and R. Belmans, "Computation of a highly saturated permanent magnet synchronous motor for a hybrid electric vehicle," *IEEE Transactions on Magnetics*, vol. 33, no. 5, pp. 4086–4088, Sept. 1997.

[3] B. Štumberger, A. Hamler, M. Trlep, and M. Jesenik, "Analysis of interior permanent magnet synchronous motor designed for flux weakening operation," *IEEE Transactions on Magnetics*, vol. 37, no. 5, pp. 3644–3647, Sept. 2001.

[4] S.I. Nabeta, A. Foggia, J.-L. Coulomb, and G. Reyne, "Finite element analysis of the skin-effect in damper bars of a synchronous machine," *IEEE Transactions on Magnetics*, vol. 33, no. 2, pp. 2065–2068, Mar. 1997.

[5] O. Drubel and R.L. Stoll, "Comparison between analytical and numerical methods of calculating tooth ripple losses in salient pole synchronous machines," *IEEE Transactions on Energy Conversion*, vol. 16, no. 1, pp. 61–67, Mar. 2001.

[6] K. Yoshida, Y. Hita, and K. Kesamaru, "Eddy-current loss analysis in PM of surface-mounted-PM SM for electric vehicles," *IEEE Transactions on Magnetics*, vol. 36, no. 4, pp. 1941–1944, July 2000.

[7] U. Pahner, S. Van Haute, R. Belmans, and K. Hameyer, "Comparison of two methods to determine the d/q-axis lumped parameters of permanent magnet machines with respect to numerical optimisation," in *Proceedings of the International Conference on Electrical Machines (ICEM98)*, Istanbul, Turkey, Sept. 1998, pp. 352–357.

[8] G. Henneberger, S. Domack, and J. Berndt, "Comparison of the utilization of brushless DC servomotors with different rotor length by 3D - finite element analysis," *IEEE Transactions on Magnetics*, vol. 30, no. 5, pp. 3675–3678, Sept. 1994.

[9] H. De Gersem, R. Mertens, U. Pahner, R. Belmans, and K. Hameyer, "A topological method used for field-circuit coupling," *IEEE Transactions on Magnetics*, vol. 34, no. 5, pp. 3190–3193, Sept. 1998.

[10] H. De Gersem, K. Debrabandere, R. Belmans, and K. Hameyer, "Motional time-harmonic simulation of slotted single-phase induction machines," accepted for publication in IEEE Transactions on Energy Conversion.